Answer to Reviewer 2

The manuscript explores a foundational question in Earth system dynamics: the capacity of the terrestrial biosphere to modulate and amplify oceanic climate signals across decadal frequencies. By employing a multi-model ensemble long equilibrium PI simulation of 11 CMIP6 models with dynamic vegetation, the authors identify a spectral reddening of the vegetation response to ENSO, specifically manifesting as a 20-25% amplification of LAI variability at multi-decadal timescales. This synthesis of partial spectral analysis and mediation frameworks provides insights for the causal chain from SST anomalies to vegetation and terrestrial carbon flux dynamics. The authors show that near-surface soil moisture acts as a hydrological integrator, subsequently amplified by internal vegetation dynamics and propose a theory for the case of non-oceanic sources of decadal climate/ecosystem predictability.

The manuscript is clearly written and easy to read. While the methodology itself is mathematically rigorous and the multi-model agreement lends significant weight to the conclusions, several critical areas require deeper theoretical and technical elaboration. I therefore recommend major revisions before the manuscript is considered for publication.

We thank the reviewer for their comments and helpful suggestions, which we have addressed in a revised version. We have uploaded a revised version as well as a version with track changes. Below, we address each of the comments (original comments in black and answers in blue).

Major comments

1. The current analytical framework focuses almost exclusively on ENSO and the PDO as the primary drivers of decadal variability. However, the Earth system contains additional important ocean–atmosphere oscillations operating on similar timescales, such as the Interdecadal Pacific Oscillation (IPO) and the Atlantic Multidecadal Oscillation (AMO). Importantly, these modes can also be influenced by ENSO variability (e.g. Dong et al. 2006; Timmermann et al. 2018). Therefore, the real-world impacts may be substantially broader and more complex than represented in the current framework. For example, ENSO may influence LAI indirectly through its modulation of IPO or AMO, while IPO and AMO themselves may also exert independent influences on LAI that are distinct from ENSO effects. The potential contributions of these additional climate modes should be evaluated and discussed. If they are currently treated as residual variability, the manuscript should quantify the magnitude of their contributions and clarify the associated uncertainties.

We thank the reviewer for raising this point. We address the IPO and AMV separately below: Regarding the IPO: Previous literature (e.g. Tung et al. 2019) has shown that the IPO is not a distinct mode of variability in the Pacific. The IPO is found to be a combination of decadal modulation of ENSO, the PDO, the AMV and external forcing. Thus, adding the IPO as a separate mediator variable would not provide new information but rather recombine variance that is already explicitly accounted for. We have now added the following lines in Section 2.2 (L. 131-133): “We note that we do not include a separate analysis of the Interdecadal Pacific Oscillation (IPO) since it has been shown that the IPO is not a distinct mode of Pacific SST variability but rather a blend of decadal-modulations of ENSO, the PDO, the AMV and externally forced warming (Tung et al. 2019).”

Regarding the AMV: We have followed the reviewer's recommendation and added a quantitative treatment of the AMV's role both as a potential independent driver of multi-decadal LAI variability and as a potential mediator or confounder of the ENSO → LAI relationship. However, we would like to note that the two papers the reviewer cites as evidence that the AMV can be influenced by ENSO (Dong et al., 2006, Timmermann et al., 2018) describe the opposite direction, namely the AMV modulating ENSO variance through tropical Atlantic SST changes and the resulting shifts in the Walker circulation. The wider literature on AMV-ENSO coupling consistently describes AMV → ENSO (e.g., Levine et al. 2017, Yu et al. 2015, Gong and Chen 2020). Some literature suggests that ENSO can affect Atlantic SSTs but these analyses focus on interannual timescales through atmospheric bridges to the tropical North Atlantic (e.g., Enfield and Mayer, 1997, Wang et al., 2017) rather than as a multi-decadal forcing of the AMV. We raise this to clarify the directionality our analyses presume, although we agree with the reviewer's comment that the AMV could nonetheless be an independent multi-decadal driver of LAI that we have not previously addressed.

We define the AMV index as the area-weighted average of detrended seasonal SST anomalies over the North Atlantic domain (0-60°N, 80°W-0°). We also did not impose an additional low-pass filter on the index, since the multi-taper analysis decomposes the spectrum at every period band (although sensitivity checks showed that applying a filter does not lead to large differences). We then performed additional analysis plotting the impact of the AMV on LAI (Fig. S5) and with the impact of ENSO removed as well as the impact of ENSO on LAI with the AMV removed (Fig. R1).

Figure S5 shows that AMV is coherent with global LAI variability at multi-decadal periods but does not produce spectral reddening. The MEM coherence squared between the AMV index and the global LAI projection on the AMV regression pattern reaches around 0.5 at periods of 50-400yr, comparable in magnitude to the ENSO-LAI coherence at long periods (Fig. 3b). However, the AMV → LAI gain is almost flat across long timescales and rather peaks at interannual periods (2-8 years). This is qualitatively different from the ENSO → LAI gain, which increases toward longer periods (Fig. 3d). The interpretation is that the AMV acts as a coherent multi-decadal forcing on vegetation, but without the active amplification that we identify for ENSO, since it is itself already exhibits red-noise-like variability. This strengthens our finding that the reddening of ENSO–driven vegetation variability is specifically a property of the vegetation to interannual variability such as ENSO.

We also test for the AMV → LAI relationship excluding the impact of ENSO (Fig. S5f-h). We find that the AMV-LAI signal at multi-decadal periods is independent of ENSO. The conditioning on the Niño3.4 index leaves the multi-decadal coherence essentially unchanged (0.5 at 50-400 yr), while the interannual coherence drops markedly. This means that the AMV drives a real, multi-decadal LAI signal that is not transmitted via ENSO, whereas the interannual part of the AMV-LAI coherence is largely shared with ENSO.

Figure R1 shows that if we look at the impact of ENSO on LAI excluding the impact of the AMV, the coherence at multi-decadal timescales and the reddening remains strong. This analysis confirms that the AMV does not mediate or confound the ENSO → LAI relationship.

We have updated the manuscript as follows:

- Abstract: "In contrast, the Atlantic Multidecadal variability (AMV) exhibits significant multi-decadal coherence with vegetation but lacks the associated spectral reddening."

- Introduction: We added the following (L. 46-48): “While the AMV is largely independent of ENSO (Zhang et al. 2019), it has been found to modulate multi-decadal ENSO variance through tropical Atlantic sea surface temperature (SST) changes and the resulting shifts in the Walker circulation (Dong et al. 2006, Levine et al. 2017).”
- Method: We added (L. 129-131): “Additionally, we test the impact of the AMV on LAI where the AMV index is calculated as the area-weighted average of detrended seasonal SST anomalies over the North Atlantic (0°-60°N, 80°W-0°).”
- Results: We added (L.387-391): “Beyond Pacific climate modes, we evaluate the role of the AMV. Although the AMV shows significant coherence with LAI at multi-decadal periods, it does not produce spectral reddening (Fig. S5). A partial spectral analysis conditioning the ENSO → LAI relationship on the AMV index further showed that the multi-decadal gain and coherence remain unchanged (not shown). These results confirm that the AMV is not the driver of the observed low-frequency amplification and does not confound the ENSO-vegetation pathway, reinforcing that the spectral reddening is a property of the ENSO-LAI system.”
- Discussion: We have removed the limitation that we did not investigate the AMV impact from the Discussion section.

References

Tung, K. K., Chen, X., Zhou, J., & Li, K. F. (2019). Interdecadal variability in pan-Pacific and global SST, revisited. *Climate Dynamics*, *52*(3), 2145-2157.

Levine, A. F., McPhaden, M. J., & Frierson, D. M. (2017). The impact of the AMO on multidecadal ENSO variability. *Geophysical Research Letters*, *44*(8), 3877-3886.

Yu, J. Y., Kao, P. K., Paek, H., Hsu, H. H., Hung, C. W., Lu, M. M., & An, S. I. (2015). Linking emergence of the central Pacific El Niño to the Atlantic multidecadal oscillation. *Journal of Climate*, *28*(2), 651-662.

Gong, Y., Li, T., & Chen, L. (2020). Interdecadal modulation of ENSO amplitude by the Atlantic multi-decadal oscillation (AMO). *Climate Dynamics*, *55*(9), 2689-2702.

Enfield, D. B., & Mayer, D. A. (1997). Tropical Atlantic sea surface temperature variability and its relation to El Niño-Southern Oscillation. *Journal of Geophysical Research: Oceans*, *102*(C1), 929-945.

Wang, L., Yu, J. Y., & Paek, H. (2017). Enhanced biennial variability in the Pacific due to Atlantic capacitor effect. *Nature communications*, *8*(1), 14887.

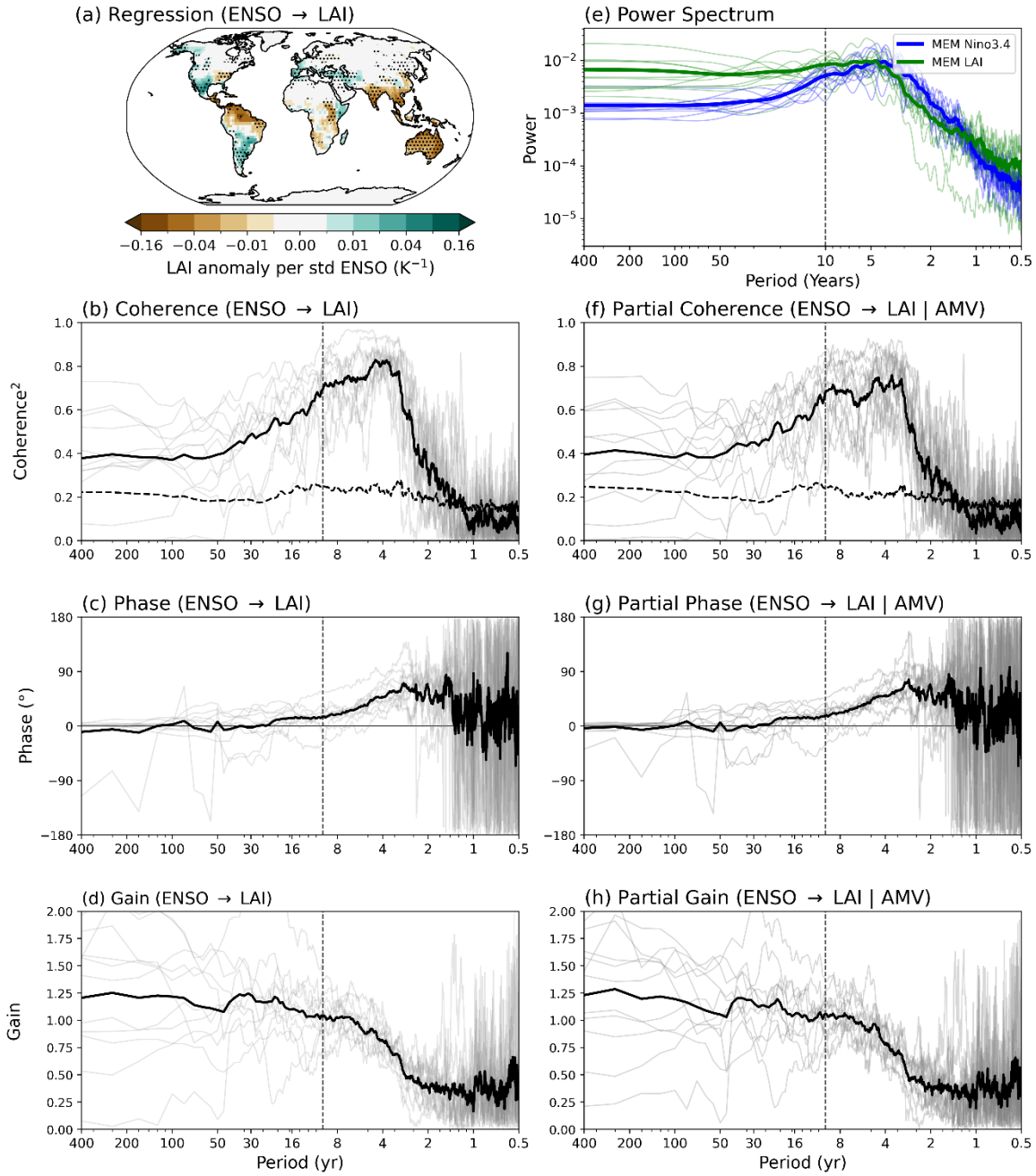

Figure R1: (a) Spatial map of the MEM regression coefficient of seasonal LAI anomalies on the Niño3.4 index, normalized by the standard deviation of the Niño3.4 index. The regression coefficient is calculated for each model based on 500 years of linearly detrended CMIP6 piControl simulations. Stippling indicates agreement on the sign of change by at least 9 of the 11 models (95% confidence). (b-d) Coherence squared, phase, and gain between the Niño3.4 index and LAI regressed on Niño3.4 in piControl. (e) Power spectrum of the Niño3.4 index (thick blue line for MEM, thin blue lines for individual models) and LAI regressed on Niño3.4 (thick green line for the MEM, thin green lines for individual models) in piControl. (f-h) Partial coherence squared, phase, and gain between the Niño3.4 index and LAI regressed on Niño3.4 in piControl, with the linear influence of the AMV index removed. In panels (b-d) and (f-h), the thick black line represents the MEM mean, and thin grey lines show individual model results. The black dashed lines in panels (b) and (f) show the critical coherence squared at the 90% significance level. The dashed vertical lines in panels (b-h) mark a period of 10 years.

2. A core weakness of the manuscript is the lack of a clear physical interpretation for "ENSO-driven decadal variability". While the statistical methods identify low-frequency power, the biological and climate-forcing features of this signal remain opaque. Based on the methodology, my understanding is that this variability (Nino 3.4 index with a 10-yr low-pass filter) primarily reflects modulation in the amplitude and/or frequency of ENSO-related SST anomalies on longer (decadal) timescales, rather than representing an independent climate mode. However, this conceptual link is not explicitly articulated in the text.

I suggest that the authors provide a clearer mechanistic framework describing how decadal-scale SST anomalies emerge from ENSO variability (e.g., through changes in ENSO amplitude, frequency, or phase asymmetry, etc.). It would also be helpful to explicitly relate these SST anomalies to the underlying climate forcing pathways that generate them.

Furthermore, the connection between these decadal SST variations and vegetation dynamics (e.g., LAI responses) should be more clearly explained. In particular, the manuscript would benefit from a clearer description of how large-scale SST variability is translated into regional hydroclimatic anomalies, and subsequently into vegetation responses, rather than treating these links implicitly.

We have now revised the Introduction and Section 3.2 to clarify that the 10-year low-pass filtered Niño3.4 index does not represent an independent decadal climate mode. Instead, it captures the decadal modulation of ENSO in amplitude, frequency and symmetry. We have added the following (L. 208-209): “Note that these filtered indices capture decadal modulations of these variables rather than representing independent climate modes.”

While the physics of these modulations are well-documented (e.g., Zhang et al. 1997, Wittenberg 2009, Sun and Yu 2009) and outside the scope of our work, our focus is instead on how this low-frequency oceanic signal is translated via atmospheric teleconnections into regional hydroclimatic anomalies and ultimately impacts vegetation. We have edited the description in the introduction to further explain how large-scale SST variability can impact vegetation (L. 30-34): “These ENSO-induced vegetation changes are primarily governed by atmospheric teleconnections that modulate regional temperature and precipitation patterns (Alessandri et al. 2008, Catalano et al. 2016). These regional anomalies then impact vegetation dynamics by altering environmental factors determining vegetation productivity, such as soil moisture and surface radiation.”

3. The concept of "memory" in soil moisture longer than its typical seasonal timescale is novel. As the authors extend this concept to decadal timescales, this leap that requires a more robust physical explanation. It is quite surprising that the process is governed by the interplay between near-surface soil water content and vegetation processes, rather than deeper soil water. Because in traditional hydrology, the deep soil and groundwater are the primary candidates for multi-year or longer memory, acting as low-pass filters that integrate high-frequency surface pulses. How this land surface coupling effectively stabilizes the anomalies, preventing their rapid dissipation and allowing the "memory" to persist across the decadal threshold should be more explicitly discussed.

We thank the reviewer for this insightful point. We wish to clarify that our results do not suggest that near-surface soil moisture (MRSOS) possesses decadal memory in isolation. Rather, our

partial spectral analysis identifies MRSOS as the critical coupling layer through which ENSO anomalies are transmitted to the vegetation.

While deep soil and groundwater are indeed the primary reservoirs for long-term water storage, our analysis shows that removing the influence of MRSOS breaks the ENSO–LAI relationship across all timescales, whereas removing the deep soil layer does not (Fig. 4). This identifies the surface layer as the functional mediator of the signal.

From a physical perspective, decadal LAI variance does not require decadal soil moisture persistence (described in L. 484-490). According to the properties of red-noise processes, a system with a response time τ concentrates half of its variance at periods longer than $2\pi\tau$ (Roe 2009). For a surface reservoir with a τ of a few months, this 2π factor shifts substantial variance into multi-annual timescales. When this signal is passed through a second integration process, which in this case is the internal vegetation response, the signal is pushed further into the decadal spectral band. The decadal memory we identify is thus a consequence of the 2π integration time combined with the soil moisture and internal vegetation dynamics.

Additionally, we would like to reiterate the limitation mentioned in our discussion (L.523-527) that while our partial spectral analysis identifies near-surface soil moisture as the proximate driver of signal reddening, it is important to recognize that shallow and deep soil layers are physically coupled. This suggests that the low-frequency memory we attribute to the near-surface may be partially supported by deeper hydrological persistence, a vertical interaction that cannot be fully disentangled using linear spectral methods. However, the method does identify near-surface soil moisture as the critical interface through which deeper soil memory is translated into the vegetation response. Ultimately, we conclude that near-surface soil moisture serves as the essential interface that translates climate-driven pulses into decadal vegetation memory by acting as the first of two sequential low-pass filters.

4. The authors completely ignore temperature influence in their analytical framework, while only considering radiation and water stress as mediators (L355). Although light and water are primary limiting factors in the tropics, temperature (thermal energy) can be the dominant control over vegetation growth in mid-latitude and high-latitude biomes. For instance, regional warming has been the primary driver of enhanced ecosystem productivity and advanced growing season phenology across the northern extratropics (e.g. Pan et al. 2015).

Crucially, ENSO systematically impacts land surface air temperature on a global scale through atmospheric teleconnections. Studies have shown that El Niño events contribute to a global-scale warming in the subsequent summer, with a strong coupling between interannual variations in the CO2 growth rate and tropical surface temperature (Wang et al. 2013). The use of a global pattern-projection index (Eq. 2) to characterize amplification is potentially "misleading" if it overlooks the temperature pathway in the 33% of the Earth's vegetated surface where temperature is the primary limiting factor (Nemani et al. 2003). If the authors intend to limit their mechanistic analysis to radiation and water stress, they should consider limiting the spatial extent of the Eq. 2 analysis strictly to the tropics (e.g. between 24S and 24N). Otherwise, the manuscript must include temperature in the mediation/partial spectral framework to justify the "global" scope of the reported decadal memory.

We had omitted temperature motivated by the dominance of water- and energy-limitation in the tropics and subtropics that contribute most to the global ENSO-vegetation pattern (Fig. 3a). However, we agree with the reviewer that ENSO has global impacts on temperatures, with these temperature changes having the potential to impact vegetation particularly at mid- to high latitudes. We have now added the analysis of ENSO → LAI excluding the impact on temperature to the supplementary Figure S6 and have added the following text to Section 3.3:

L. 396-399: "Additionally, temperature can be the dominant control over vegetation growth in mid- and high-latitude biomes (Nemani et al. 2003). Consequently, we focus on four key variables, namely surface downwelling shortwave radiation (RSDS), near-surface soil moisture (MRSOS), deep-layer soil moisture (total soil moisture content MRSO minus MRSOS) and near-surface air temperature (TAS)."

L. 408-411: "In contrast, excluding near-surface air temperature still gives statistically significant partial coherence across annual to multi-decadal timescales and a persistent spectral reddening. Thus, both radiation and shallow soil moisture could be more critical mediators in the propagation of the ENSO signal to vegetation on a global scale than temperature, although inter-model spread persists."

Minor comments

1. L99 please elaborate on the two-way feedbacks commonly included in the models.

We have expanded this section to explain what the two-way feedbacks consist of as follows (L. 103-105): "Specifically, climate and its variability impact LAI by governing the availability of water, light, and thermal energy required for photosynthesis and phenology, while LAI in turn can modify the climate via changes in albedo, evapotranspiration, and aerodynamic roughness."

2. Please specify whether this data was obtained from a single unique realization per model, or if multiple initial-condition ensemble members of 1 model were used to robustly characterize internal variability.

We used a single piControl realisation per model since the long timeseries (500 years) helps to characterise internal variability, in an analogous way to how multiple ensemble members help to characterize internal variability in shorter historical simulations. We have updated L. 90-92: "To isolate and analyze the low-frequency variability of the coupled ocean-atmosphere-land-vegetation system, we utilize single piControl realisations from 11 ESMs participating in the Coupled Model Intercomparison Project Phase 6 (CMIP6) (Eyring et al. 2016)."

3. L131 (Eq 2): The pattern-projection index Tv represents global vegetation anomalies as a single collapsed scalar time series. While this isolates the temporal evolution of a specific mode, it risks obscuring regional features due to spatial cancellation—where out-of-phase land anomalies (such as tropical drying counteracted by high-latitude greening) smooth out the global signal. To evaluate how representative Tv truly is of decentralized global dynamics, it would be

highly valuable to loop the coherence and gain calculations across individual grid cells. Plotting global gridcell-level maps of spectral coherence and gain directly against the oceanic index would provide a more robust, straightforward, and geographically interpretable picture of terrestrial memory hotspots.

We thank the reviewer for this suggestion and agree that a gridcell-level map of spectral coherence and gain is a valuable complement to the global T_V index to identify regional hotspots. We would like to note nonetheless that the projection in Eq. 2 already weights each gridcell by its regression coefficient, so out-of-phase contributions are not simply averaged.

We have now added a new supplementary figure (new Fig. S2) which shows the MEM gridcell-level coherence squared and gain between the Nino3.4 index and LAI in piControl, evaluated over an interannual (2-4 years) and decadal and longer (>10 years) period band. Methodologically, the new figure repeats the multi-taper spectral analysis of Fig. 3 at every land grid cell rather than on the global T_V projection. For each of the 11 CMIP6 models, we load the same normalised Niño3.4 index used throughout the manuscript and the corresponding piControl LAI field (with identical seasonal-anomaly, detrending and land-masking preprocessing as in Fig. 3). At every land grid cell, we standardise the LAI time series by its local standard deviation and compute the MTM coherence squared and gain spectrum against Niño3.4. We then average each spectrum within the two period bands and take the multi-model mean. A third row of the figure shows the MEM gain multiplied by the sign of the MEM regression coefficient at each grid cell, in order to distinguish negative anomaly hotspots (brown) from positive ones (green). Stippling on the signed-gain row indicates where at least 9 of the 11 models agree on the sign of the regression, matching the convention used elsewhere in the manuscript.

This figure shows that the coherence ENSO-LAI signal is primarily concentrated in the tropics/subtropics, specifically Amazonia and Southeast Asia, with much weaker coherence over mid and high-latitude regions like Alaska and the Central USA. Thus, the global T_V index is picking up the same geographic hotspots that the gridcell analysis identifies. Additionally, Figure S2 shows the strong reddening of the signal (i.e. low to high gain values) from interannual to decadal and longer timescales, peaking mainly over the tropical regions like Amazonia, SE Asia, eastern Australia and the Congo. This is the same reddening seen in the global T_V gain (Fig. 3d), now resolved geographically. The signed-gain map at decadal-and-longer periods reproduces the spatial pattern of the time-domain regression in Fig. 3a, with brown responses over Amazonia, northern Australia, India and SE Asia, and green responses over Argentina and parts of East Africa, with model agreement (stippling) over essentially the same tropical/subtropical band. This also demonstrates that the multi-decadal memory respects the same ENSO teleconnection geography as the underlying interannual response, rather than activating different mechanisms in different regions.

We have added the following description to Section 3.2 (L. 359-368): “To identify the geographical drivers of this global signature, we first conducted a gridcell-resolved analysis (Fig. S2), which confirms that the strongest coherence and reddening are concentrated in tropical hotspots like Amazonia and Southeast Asia. By resolving the signal at each pixel, we verify that the global T_{LAI} pattern reflects real local dynamics rather than an artifact of spatial cancellation between out-of-phase regional anomalies. These findings are supported by targeted regional spectral analysis of the major tropical rainforest regions (Amazon, Congo and Southeast Asia), which dominate global vegetation productivity and are strongly influenced by ENSO (Fig. S3). While the gains from this regional analysis are not directly comparable to the gain in the global T_{LAI} index in a quantitative sense, the qualitative behavior in the Amazon and Southeast Asia shows

pronounced spectral reddening and significant decadal coherence, mirroring the global amplification pattern. In contrast, the Congo region shows no coherence on long timescales, which might be related to low model agreement in this region (Fig. 3a)."

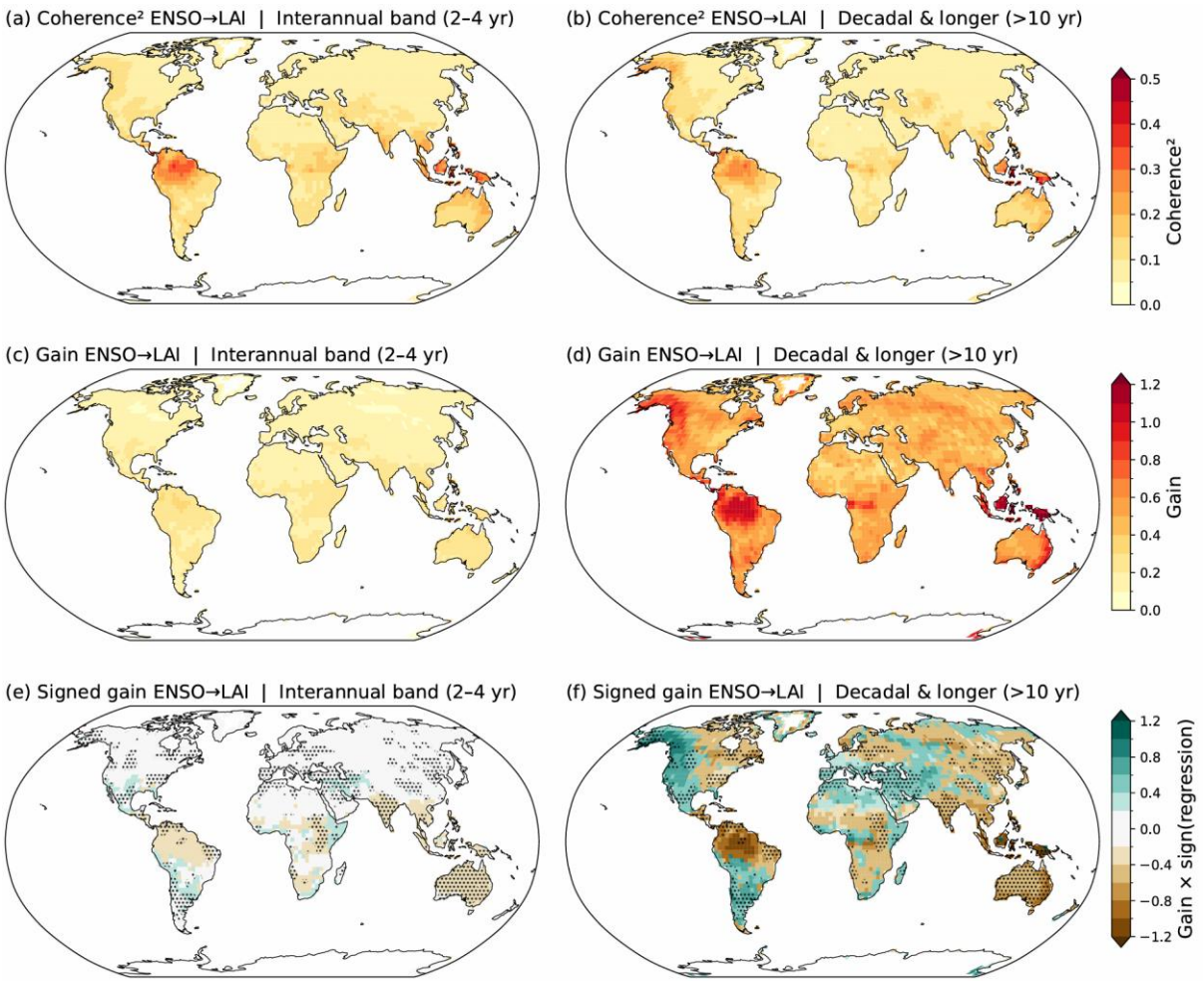

Fig. S2: Gridcell-level MEM of (a, b) coherence squared and (c, d) gain magnitude between the Niño3.4 index and LAI in piControl, evaluated in the (left column) interannual 2–4 yr period band and (right column) decadal-and-longer > 10 yr period. Subplots (e, f) show the gain magnitude multiplied by the sign of the MEM regression coefficient (Fig. 3a), so that negative (brown) and positive (green) vegetation anomaly hotspots can be distinguished. Stippling in (e, f) indicates where at least 9 of the 11 models agree on the sign of the regression. LAI at each grid cell is standardised by its local standard deviation prior to the spectral analysis, so the gain values are directly comparable to the global T_v gain in Fig. 3d.